Aluminum-doped zinc oxide as anode for organic near-infrared photodetectors

2014 J. Phys. D: Appl. Phys. 47 335104

(http://iopscience.iop.org/0022-3727/47/33/335104)

IOP Publishing Journal of Physics D: Applied Physics
J. Phys. D: Appl. Phys. **47** (2014) 335104 (5pp) doi:10.1088/0022-3727/47/33/335104

Aluminum-doped zinc oxide as anode for organic near-infrared photodetectors

Xing Wang[2,3,5], Fang Fang[1,2,4,5], Zisheng Su[3,4], Xuan Fang[2], Guang Zhang[3], Junbo Wang[3], Zhipeng Wei[2], Jinhua Li[2] and Xiaohua Wang[2]

[1] Nanchang University, No 235 East Nanjing Road, Jiangxi Province, Nanchang 330047, People's Republic of China
[2] State Key Laboratory of High Power Semiconductor Laser, School of Science, Changchun University of Science and Technology, Changchun 130022, People's Republic of China
[3] State Key Laboratory of Luminescence and Applications, Changchun Institute of Optics, Fine Mechanics and Physics, Chinese Academy of Sciences, Changchun 130033, People's Republic of China

E-mail: fang_fang0131@126.com (F Fang) and suzs@ciomp.ac.cn (Z Su)

Received 24 April 2014, revised 16 June 2014
Accepted for publication 23 June 2014
Published 25 July 2014

Abstract

High transparency and low resistivity aluminum-doped zinc oxide (AZO) films were prepared by atomic layer deposition. The AZO films show a transparency of about 80% in the near-infrared (NIR) region and a resistivity of the order of 10^{-3} Ω cm. Organic small molecule NIR-photodetectors (NIR-PDs) with AZO as the anode have been demonstrated for the first time with lead phthalocyanine (PbPc) and C_{60} as the donor and acceptor, respectively. The optimized NIR-PD exhibited an external quantum efficiency of 6.2% at 760 nm. This result indicated that AZO can be used as the anode for high efficiency NIR-PDs.

Keywords: aluminum-doped zinc oxide, atomic layer deposition, photodetectors

(Some figures may appear in colour only in the online journal)

1. Introduction

Organic photodetectors (PDs) have been the subjects of extensive research because of their large-area detection, wide selection of materials and compatibility with flexible substrates [1, 2]. Near-infrared PDs (NIR-PDs) have tremendous potential in industrial and scientific applications, such as remote control, night vision, chemical/biological sensing, optical communication, and spectroscopic and medical instruments [3–10]. Indium tin oxide (ITO) is commonly used as the anode for organic electronic devices due to its high conductivity, work function and transparency in the visible to NIR spectral range [11, 12]. However, indium is a relatively scarce element in the Earth's crust, which increases the cost of the devices. Moreover, indium is also a hazardous threat to the environment and human health. The indium of ITO layer can diffuse into the organic layers, leading to degradation of the devices [13]. Thus it is desired to find other low cost and nontoxic materials with similar optical and electrical properties to replace ITO.

Zinc oxide (ZnO) is a wide and direct band gap semiconductor material that has received considerable attention in recent years [14–17]. The main advantages of ZnO compared with ITO are that it is nontoxic, inexpensive and more stable in reducing ambient.

An n-type conductivity of ZnO can be increased by doping with a trivalent atom, such as aluminum (Al), gallium or indium [16]. Among these materials, Al-doped ZnO (AZO) has been considered as a suitable electrode for optoelectronic devices owing to its lowest resistivity and excellent optical transparency in the visible and NIR regions. AZO has been used as the anode for organic light-emitting diodes and organic solar cells [18–22]. However, it has not been used in organic PDs, as far as we know. AZO films can be deposited by different techniques, such as sol–gel coating [23], chemical vapour deposition [24], pulsed laser deposition [18], radio-frequency sputtering [19, 20] and atomic layer deposition (ALD) [25–27]. ALD is a promising deposition technique for semiconductor films since it has several practical advantages

[4] Authors to whom any correspondence should be addressed.
[5] These authors contributed equally to this work.

including accurate and simple thickness control, large area and large batch capability, good conformality and reproducibility. The films prepared by ALD are usually dense, pinhole-free and extremely conformal to the underlying substrate. Recently, ALD technology has been employed to grow transparent conductive AZO films with resistivity as low as of the order of $10^{-4}\,\Omega\,\mathrm{cm}$ [16].

In this work, AZO films deposited by ALD were used as the anode for organic small molecule NIR-PDs. Lead phthalocyanine (PbPc) was a shuttlecock-shaped molecule and has received attention recently in the field of organic photovoltaic devices because of its high absorption coefficient at the NIR wavelength region [28, 29]. Herein, PbPc and C_{60} were chosen as the donor and acceptor phases for the NIR-PDs, respectively. The optimized NIR-PD exhibited an external quantum efficiency (EQE) of 6.2% at 760 nm.

2. Experiments

AZO films were deposited on glass substrates. Before the film deposition, the substrate was cleaned through the Radio Corporation of America process, and the substrate was treated by ultrasonic cleaning in alcohol and acetone sequentially. The ALD equipment is a 6 inch small chamber LabNano™9100 ALD system from Ensure NanoTech (BeiJing). Diethylzinc ($(C_2H_5)_2Zn$, DEZn) and tri-methyl aluminum ($Al(CH_3)_3$, TMA) were used as the metal precursors for ZnO and Al_2O_3, respectively, while water vapour was used as the oxidant. During the ALD process, the DEZn and TMA sources were not intentionally heated. Nitrogen (99.999%) was used as carrier and purge gas with a flow rate of 20 sccm. During the deposition, the substrates were kept at 170 °C. The total ALD cycles of the multilayers were 1000 and the ratio of the ALD cycles of ZnO and Al_2O_3 sublayers varied, with 49 : 1, 23 : 1 and 15 : 1 corresponding to the Al concentration of 1%, 2% and 3% (hereafter denoted as AZO1, AZO2 and AZO3), respectively. The thickness of the AZO films was about 200 nm.

The NIR-PDs were fabricated on AZO substrates via shadow masks to form devices (schematic diagram of the structure for the detector is shown in figure 1). The substrates were routinely cleaned followed by ultraviolet (UV)–ozone treatment for 10 min. The NIR-PDs have a structure of substrate/PbPc (60 nm)/C_{60} (60 nm)/Al (100 nm), where PbPc and C_{60} acted as the donor and acceptor, respectively. The organic layers and Al cathode were sequentially deposited on the substrates by thermal evaporation in a vacuum chamber at a pressure of 5×10^{-4} Pa without breaking vacuum.

X-ray diffraction (XRD) patterns were measured with a diffractometer (Rigaku D/Max-2500) using Cu Kα radiation ($\lambda = 1.540\,56$ Å). Surface morphologies of the films were measured on a scanning electron microscopy (SEM) (Hitachi S4800). Absorption spectra were recorded on a spectrophotometer (Lambda 950). Electrical characteristics were measured by Lakeshore Vsm707. EQE spectra were obtained with a lock-in amplifier (Stanford SR803) under monochromatic illumination at a chopping frequency of 130 Hz by a chopper (Stanford SR540). All measurements were carried out under ambient conditions.

Figure 1. Schematic diagram of the structure of our planar heterojunction NIR-PD glass(AZO)/PbPc/C_{60}/Al.

3. Results and discussion

Figure 2(*a*) shows the normalized XRD patterns of the AZO and ZnO films. The XRD pattern of pure ZnO film exhibited multiple crystalline ZnO structure with (1 0 0), (0 0 2) and (1 1 0) diffraction peaks [16]. With the Al concentration increased, the value of (0 0 2) peak intensity compared with (1 0 0) peak was reduced. The Al_2O_3 layer deposited by ALD was amorphous at the growth temperature of <250 °C, so the decrease of the diffraction peaks at higher Al concentration can be explained by the fact that the amorphous Al_2O_3 doping layers destroyed the crystal quality during the growth of AZO films. Moreover, we calculated the sizes by Scherrer formula:

$$D = K\lambda/\beta\cos\theta$$

where D is the crystallite size, K is a constant, λ is the x-ray wavelength of the Cu target, β is the full-width at half-maxima (FWHM) and θ is the diffraction angle. The FWHM of (0 0 2) peak was increased from 0.19° to 0.93°, while the estimated crystallite size along *c*-axis decreased from 50.48 to 10.43 nm (as shown in figure 2(*b*)). As we could see from the SEM images (figure 3), with the Al concentration increased from 1% to 3%, the crystal size reduced, which was consistent with the XRD results.

Figure 4 showed the transmission spectra of the AZO films; for reference, the transmission spectrum of ITO was also provided. The AZO films exhibited a lower transmission in the UV region, which could be attributed to the slightly lower band gap of the AZO films with low doping concentration of Al [16]. However, the transmission of all the AZO films was higher than 80% in the visible region and 75% in the NIR region, which was comparable to the ITO film. These properties allowed the AZO film as a potential alternative to ITO for anode use in organic NIR-PDs system.

The electrical property of the anode plays an important role in determining the performance of optoelectronic devices. Table 1 lists the electrical characteristics of the AZO films. The resistivity, carrier density, and motility of the films were measured by Hall effect measurement, while the sheet resistances were calculated from their resistivities and thicknesses. The resistivity of AZO1 was $1.52 \times 10^{-2}\,\Omega\,\mathrm{cm}$. With the increase of Al doping concentration from 0 to 2%, the resistivity of the AZO films is significantly reduced. When the Al concentration went up to 2%, the resistivity of AZO films reduced to $6.38 \times 10^{-3}\,\Omega\,\mathrm{cm}$. However, as for 3% Al concentration, the resistivity increased to $8.30 \times 10^{-3}\,\Omega\,\mathrm{cm}$. The most probable evidence of increase of the resistivity

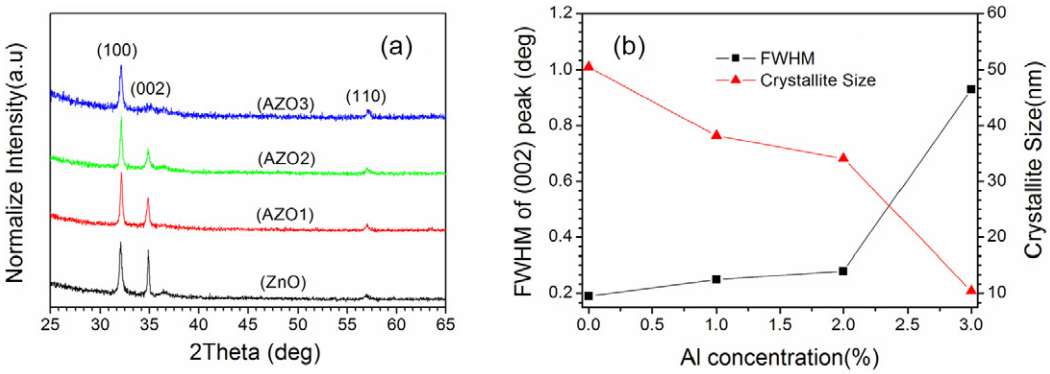

Figure 2. (*a*) XRD patterns of AZO and ZnO films. (*b*) The left axis represents the dependence of the FWHM of the AZO films (0 0 2) peak on the Al concentration (black square) and the right axis is the estimated crystallite size along *c*-axis (red triangle).

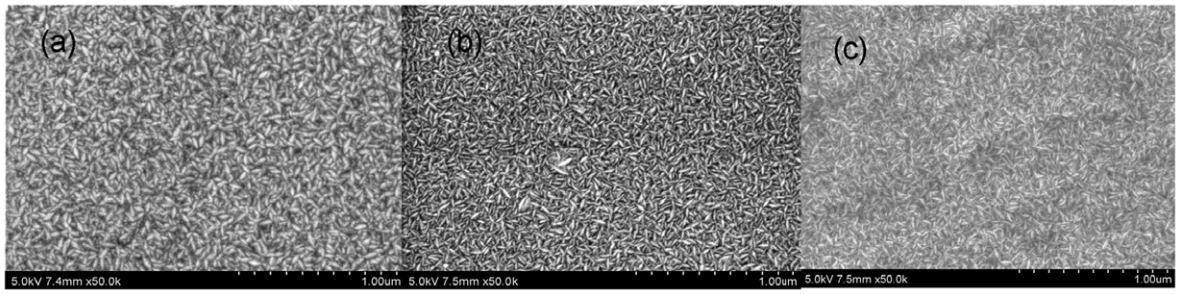

Figure 3. SEM image of different Al concentration AZO films: (*a*) 1% Al concentration, (*b*) 2% Al concentration, (*c*) 3% Al concentration.

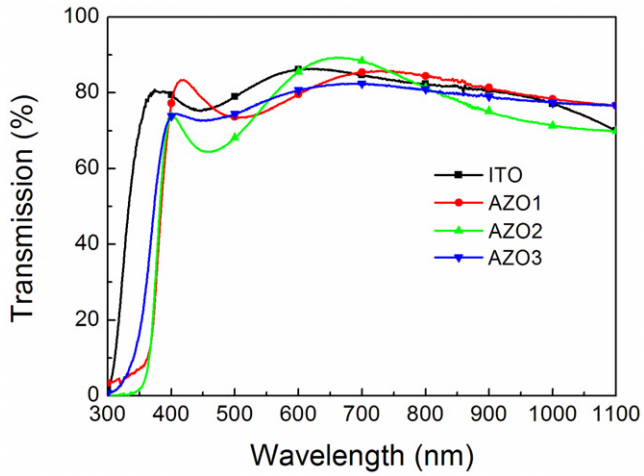

Figure 4. Transmission spectra of ITO and AZO films.

from 2% to 3% is the crystallinity: when the crystallinity of films becomes worse or more amorphous, the resistivity also increases. This effect also happens during the concentration change from 0% to 2%, but at this range the doping is the dominant process. The low resistivity of the AZO films makes them more suitable to be used as the anode for organic NIR-PDs.

Before the construction of the NIR-PDs, the absorption spectra of the PbPc films were investigated. Figure 5 describes the absorption spectra of the 60 nm PbPc films on different substrates. All the PbPc films showed a broad band absorption in the NIR region with a peak at about 730 nm and a shoulder

Table 1. Electrical characteristics of the AZO and ZnO films.

Films	Resistivity (Ω cm)	Carrier density (n cm^{-3})	Mobility (cm^2 V^{-1} s^{-1})
AZO1	1.52×10^{-2}	4.70×10^{19}	8.72
AZO2	6.38×10^{-3}	1.96×10^{20}	5.00
AZO3	8.30×10^{-3}	1.43×10^{20}	5.25
ZnO	4.36×10^{-1}	1.41×10^{19}	1.02

at about 900 nm. It was reported that PbPc with a triclinic phase was formed during the later stage of growth (>20 nm), whereas the monoclinic phase was formed during the initial growth (<10 nm) of a relatively thick film [28, 29]. The former absorption could be assigned to the amorphous or monoclinic phases, while the latter to the triclinic phase [30].

Figure 6 depicts the EQE spectra of the NIR-PDs fabricated on different AZO substrates and ITO. The EQE spectra of the PDs exhibited a broad band response in the NIR region with a peak at about 760 nm. The EQE of the PDs increased with the Al doping concentration in the AZO films, and a highest EQE of 6.2% at 760 nm was found for the PD on AZO2 anode. This effect is attributed to the reduced resistance with Al doping, as listed in table 1. It can be noted that there is an obvious difference between the spectral shapes of the EQE and absorption. The shape of the EQE spectrum highly depends on the optical field distribution in the device. For a thick PbPc film, a triclinic phase is formed during the later stage of growth (>20 nm), whereas the monoclinic phase is formed during the initial growth (<10 nm), corresponding to the absorption at about

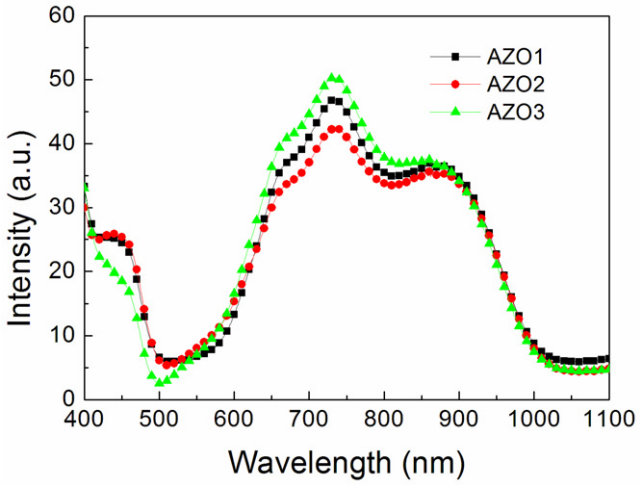

Figure 5. Absorption spectra of 60 nm PbPc films on different AZO substrates.

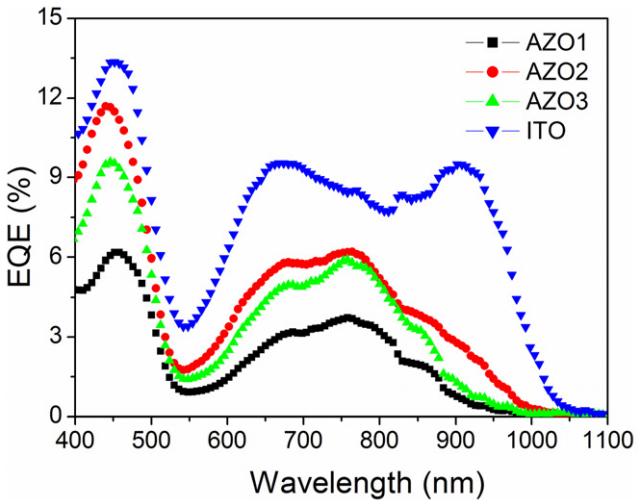

Figure 6. EQE spectra of NIR-PDs on different AZO substrates.

900 nm and 730 nm, respectively. Thus we speculate that the optical field distribution of the NIR-PDs on AZO is favourable for more excitons of monoclinic phase of PbPc to diffuse to the PbPc/C_{60} interface and then dissociate to form the charge carriers, which results in the differences between EQE and absorption spectral shapes. Further works are ongoing to understand these phenomena and their mechanisms. The EQE spectrum of the NIR-PD on ITO shows two peaks at about 650 and 900 nm. The different EQE spectra on NIR-PDs on AZO and ITO may be attributed to the different optical field distributions resulting from their different refractive indexes. The EQE of the PD at 760 nm is 8.7%, which is a little higher than that on AZO substrates. The lower EQE of AZO based PDs is attributed to the higher resistivity of AZO. Although at the current stage of technology, the resistivity of the AZO films remains to be improved, considering the inherent advantages of AZO as a nontoxic, inexpensive, and more stable alternative anode material, we still have faith that the higher EQE can be expected by further optimizing the deposition technology of the AZO film and the device structure of the NIR-PD.

4. Summary

In summary, high transparency and low resistivity AZO films were prepared by ALD method. The transparency of the AZO films is about 80% in the NIR region and the resistivity is of the order of $10^{-3}\,\Omega\,\mathrm{cm}$. Such properties make them suitable to replace ITO as the anode for organic NIR-PDs. NIR-PDs were successfully realized with a simple PbPc/C_{60} planar heterojunction as the active layers. The optimized PD exhibited an EQE of 6.2% at 760 nm at zero bias. These findings indicated the promise of AZO film as a low cost and environment friendly anode material for organic NIR-PDs.

Acknowledgments

This work is supported by the National Natural Science Foundation of China (61204065, 61307045, 61107082 and 11004187), Research Fund for the Doctoral Program of Higher Education of China (20112216120005), the Developing Project of Science and Technology of Jilin Province (201201116) and National Key Lab of High Power Semiconductor Lasers Foundation (No 9140C310101120C031115).

References

[1] Dong H, Zhu H, Meng Q, Gong X and Hu W 2012 *Chem. Soc. Rev.* **41** 1754
[2] Baeg K J, Binda M, Natali D, Caironi M and Noh Y Y 2013 *Adv. Mater.* **25** 4267
[3] Gong X, Tong M, Xia Y, Cai W, Moon J S, Cao Y, Yu G, Shieh C L, Nilsson B, and Heeger A J 2009 *Science* **365** 1665
[4] Yao Y, Liang Y, Shrotriya V, Xiao S, Yu L and Yang Y 2007 *Adv. Mater.* **19** 3979
[5] Qian G, Qi J, Davey J A, Wright J S and Wang Z Y 2012 *Chem. Mater.* **24** 2364
[6] Liu X, Wang H, Yang T, Zhang W, Hsieh I F, Cheng S Z D and Gong X 2012 *Org. Electron.* **13** 2929
[7] Zimmerman J D, Diev V V, Hanson K, Lunt R R, Yu E K, Thompson M E and Forrest S R 2010 *Adv. Mater.* **22** 2780
[8] Binda M, Iacchetti A, Natali D, Beverina L, Sassi M and Sampietro M 2011 *Appl. Phys. Lett.* **98** 073303
[9] Wang J B, Li W L, Chu B, Lee C S, Su Z S, Zhang G, Wu S H and Yan F 2011 *Org. Electron.* **12** 34
[10] Wu S H, Lo M F, Chen Z Y, Ng T W, Hu X, Mo H W, Wu C, Li W L and Lee C S 2012 *Phys. Status Solidi RRL* **6** 129
[11] Armstrong N R, Veneman P A, Ratcliff E, Placencia D and Brumbach M 2009 *Acc. Chem. Res.* **42** 1748
[12] Xiang C Y, Koo W, So F, Sasabe H and Kido J 2013 *Light: Sci. Appl.* **2** 74
[13] Lee S T, Gao Z Q and Hung L S 1999 *Appl. Phys. Lett.* **75** 1404
[14] ÖzgürÜ, Alivov Y I, Liu C, Teke A, Reshchikov M A, Doğan S, Avrutin V, Cho S J and Morkoç H 2005 *J. Appl. Phys.* **98** 041301
[15] Fang F, Zhao D X, Li BH, Zhang Z Z, Shen D Z and Wang X H 2010 *J. Phys. Chem* C **114** 12477
[16] Fang F, Zhao D X, Fang X, Li J H, Wei Z P, Wang S Z, Wu J L and Wang X H 2011 *J. Mater. Chem.* **21** 14979
[17] Lai Y Y, LanY P and Lu T C 2013 *Light: Sci. Appl.* **2** e76
[18] Kim H, Gilmore C M, Horwitz J S, PiquéA, Murata H, Kushto G P, Schlaf R, Kafafi Z H and Chrisey D B 2000 *Appl. Phys. Lett.* **76** 259
[19] Jiang X, Wong F L, Fung M K and Lee S T 2003 *Appl. Phys. Lett.* **83** 1875

[20] Murdoch G B, Hinds S, Sargent E H, Tsang S W, Mordoukhovski L and Lu Z H 2009 *Appl. Phys. Lett.* **94** 213301
[21] Gong S C, Jang J G, Chang H J and Park J S 2011 *Synth. Met.* **161** 823
[22] Saarenpää H, Niemi T, Tukiainen A, Lemmetyinen H and Tkachenko N 2010 *Sol. Energy Mater. Sol. Cells* **94** 1379
[23] Mathur S, Veith M, Haas M, Shen H, Lecerf N, Huch V, Hüfner S, Haberkorn R, Beck H P and Jilavi M 2001 *J. Am. Ceram. Soc.* **84** 1921
[24] Volintiru I, Creatore M, Kniknie B J, Spee C I M A and vande Sanden M C M 2007 *J. Appl. Phys.* **102** 043709
[25] Luka G, Godlewski M, Guziewicz E, Stakhira P, Cherpak V and Volynyuk D 2012 *Semicond. Sci. Technol.* **27** 074006
[26] Chen X Y, Li J H, Sun Z H, Fang X, Wei Z P, Fang F, Chu X Y, Li S and Wang X H 2013 *J. Alloys Compounds* **571** 114
[27] Dhakal T, Nandur A S, Christian R, Vasekar P, Desu S, Westgate C, Koukis D I, Arenas D J and Tanner D B 2012 *Sol. Energy* **86** 1306
[28] Zhao W, Mudrick J P, Zhang Y, Hammond W T, Yang Y and Xue J 2012 *Org. Electron.* **13** 129
[29] Kim H J, Shim H S, J Kim W, Lee H H and Kim J J 2012 *Appl. Phys. Lett.* **100** 263303
[30] Vasseur K, Rand B P, Cheyns D, Froyen L and Heremans P 2011 *Chem. Mater.* **23** 886